



HAL
open science

Steroidogenic Factor-1 Lineage Origin of Skin Lesions in Carney Complex Syndrome

Isabelle Sahut-Barnola, Anne-Marie Lefrançois-Martinez, Damien Dufour, Jean-Marie Botto, Crystal Kamilaris, Fabio Faucz, Constantine Stratakis, Pierre Val, Antoine Martinez

► **To cite this version:**

Isabelle Sahut-Barnola, Anne-Marie Lefrançois-Martinez, Damien Dufour, Jean-Marie Botto, Crystal Kamilaris, et al.. Steroidogenic Factor-1 Lineage Origin of Skin Lesions in Carney Complex Syndrome. *Journal of Investigative Dermatology*, 2022, 142 (11), pp.2949-2957.e9. 10.1016/j.jid.2022.04.019 . hal-03869040

HAL Id: hal-03869040

<https://cnrs.hal.science/hal-03869040>

Submitted on 24 Nov 2022

HAL is a multi-disciplinary open access archive for the deposit and dissemination of scientific research documents, whether they are published or not. The documents may come from teaching and research institutions in France or abroad, or from public or private research centers.

L'archive ouverte pluridisciplinaire **HAL**, est destinée au dépôt et à la diffusion de documents scientifiques de niveau recherche, publiés ou non, émanant des établissements d'enseignement et de recherche français ou étrangers, des laboratoires publics ou privés.



Distributed under a Creative Commons Attribution - NonCommercial - NoDerivatives 4.0 International License

Steroidogenic factor-1 lineage origin of skin lesions in Carney complex syndrome

Isabelle SAHUT-BARNOLA¹, A-Marie LEFRANCOIS-MARTINEZ¹, Damien DUFOUR¹,
Jean-Marie BOTTO², Crystal KAMILARIS³, Fabio R. FAUCZ³, Constantine A.
STRATAKIS³, Pierre VAL¹, Antoine MARTINEZ^{1α}

¹ *i*GReD, CNRS, Inserm, Université Clermont-Auvergne, France

² Global Skin Research Center, Ashland, Sophia Antipolis, France

³ SEGEN, NICHD, NIH, Bethesda, MD

^αCorrespondence: *i*GReD, CNRS UMR6293, INSERM U1103, Faculté de Médecine, CRBC,
Université Clermont-Auvergne, 28 place Henri Dunant, TSA 50400, 63001 Clermont-Ferrand,
France. Tel : +33473407409 ; E-mail: antoine.martinez@uca.fr

Short title: mouse model for skin lesions of Carney syndrome

ABSTRACT

Carney complex (CNC) is a rare familial multi-neoplastic syndrome predisposing to endocrine and non-endocrine tumors due to inactivating mutations of *PRKARIA* leading to perturbations of the cAMP protein kinase A (PKA) signaling pathway. Skin lesions are the most common manifestation of CNC, including lentigines, blue nevi and cutaneous myxomas, in unusual locations such as oral and genital mucosa. Unlike endocrine disorders, the pathogenesis of skin lesions remains unexplained. Here, we show that embryonic invalidation of the *Prkar1a* gene in Steroidogenic Factor-1-expressing cells, leads to the development of familial skin pigmentation alterations reminiscent of those in patients. Immunohistological and molecular analyses coupled with genetic monitoring of recombinant cell lineages in mouse skin, suggest that familial lentiginosis and myxomas occurs in skin areas specifically enriched in dermal melanocytes. In lentigines and blue nevi-prone areas from mutant mice and patients, *Prkar1a/PRKARIA* invalidation occurs in a subset of dermal fibroblasts capable of inducing, under the influence of PKA signaling, the production of pro-melanogenic EDN3 and HGF signals. Our model strongly suggests that the origin of the typical CNC cutaneous lesions is the result of non-cell-autonomous pro-melanogenic activity of a dermal fibroblast population sharing a community of origin with SF-1 lineage.

INTRODUCTION

Carney complex (CNC) is a rare multiple endocrine neoplasia and lentiginosis syndrome, that is familial in 70% of cases, with autosomal dominant inheritance. CNC is characterized by pigmented lesions of the skin and mucosal, myxomas (of the heart, skin and breast) and various endocrine and non-endocrine tumors. Endocrine manifestations of CNC affect the adrenal cortex (25-68% of cases), gonads (testes 35-41%, ovaries 14%), pituitary and thyroid (up to 70%). CNC patients may also present with cardiac myxoma (20-40%) and skin myxoma (20-

1
2
3 50%). The most common clinical manifestation is abnormal skin pigmentation (60-80%)
4
5 ranging from lentigines or so called freckles to blue nevi (Correa et al. 2015; Stratakis 2016;
6
7 Espiard et al. 2020). Lentigines observed in CNC patients are found in unusual places such as
8
9 the cheeks, vermilion border, ears, eyelids and/or genitals. In contrast to endocrine
10
11 manifestations, the pathogenesis of cutaneous disorders remains unexplained. CNC is primarily
12
13 caused by inactivating mutations of the *PRKARIA* gene encoding the R1 α subunit of protein
14
15 kinase A (PKA), resulting in constitutive activation of cyclic adenosine monophosphate
16
17 (cAMP)-PKA signaling pathway (Carney et al. 1985; Casey et al. 2000; Kirschner et al. 2000).
18
19

20
21
22 We have previously developed genetic mouse models carrying conditional *Prkar1a*
23
24 invalidation using different Cre drivers (*Akr1b7-Cre*, *AS^{Cre}* and *Sfl-Cre*) allowing spatio-
25
26 temporal R1 α loss in steroidogenic cells (Sahut-Barnola et al. 2010; Drelon et al. 2016;
27
28 Dumontet et al. 2018; Amaya et al. 2021). These models recapitulated the primary bilateral
29
30 adrenocortical hyperplasia observed in CNC patients, associated with chronic glucocorticoid
31
32 excess (Cushing's syndrome), which resulted in metabolic comorbidities and alterations of
33
34 brain structure. Remarkably, spotty skin pigmentation, the most common and earliest clinical
35
36 manifestation of CNC, was only observed when *Prkar1a* was invalidated using the *Sfl-Cre*
37
38 driver (*Prkar1a^{f/f}::Sfl-Cre⁺*, named AdKO_{2.0}) that was active in steroidogenic cell lineage
39
40 from E10.5-E11.5 onwards (Bingham et al. 2006). Here we show that AdKO_{2.0} mice exhibit
41
42 skin alterations characterized by hyperpigmentation in skin areas mirroring those of CNC
43
44 patients, including lentigines, blue nevi and development of cutaneous myxomas. We used
45
46 immunohistological and molecular approaches as well as cell lineage tracing studies to
47
48 characterize the origin and pathogenesis of these cutaneous lesions in AdKO_{2.0} mice and
49
50 compared them to skin biopsies from CNC patients. Here, we show that AdKO_{2.0} mice
51
52 recapitulate skin lesions found in CNC patients and allow to identify non-cell-autonomous
53
54 mechanisms involving specific dermal cell population.
55
56
57
58
59
60

1
2
3
4
5 **RESULTS AND DISCUSSION**
6
7

8 **Pigmented skin lesions in AdKO_{2.0} mice are correlated with *Sfl-Cre* driver activity.** The
9

10 skin pigmentation phenotype of AdKO_{2.0} mice was detected at birth as a pigmented ring around
11 the eyes. In five-day-old AdKO_{2.0} mice, hyperpigmentation was found in the perigenital skin,
12 tail and around the nipples in female. Hyperpigmentation also formed discrete symmetrical
13 patches under the jaw and on the joints of the upper limbs (Figure 1a-b, Figure S1a). These skin
14 manifestations, reminiscent of lentiginos, were fully penetrant and always found in these
15 specific areas. Since adult AdKO_{2.0} mice had glucocorticoid-induced alopecia, this pattern of
16 lentiginos remained visible despite hair growth, as large areas around the nipples, spotty
17 pigmentation on the scrotum and at the upper limb junctions (Figure S1b). Fontana Masson
18 (FM) staining was carried out on skin sections from differentially pigmented areas in 5 days
19 mice. As expected, there were no melanin pigments or histological alterations in the abdominal
20 skin regardless of wild-type (WT) and AdKO_{2.0} mice. By contrast, melanin staining in the
21 dermis (at least papillary and upper reticular dermis) was strongly increased in genitalia skin
22 sections from AdKO_{2.0} mice compared to WT (Figure 1c, top panels). The specific
23 hyperpigmentation of AdKO_{2.0} mutants does not rely on the systemic action of excess
24 glucocorticoids, as the other two adrenal-specific *Prkar1a* invalidation models using *Akr1b7-*
25 *Cre* (AdKO) or *AS^{Cre}* (DAdKO) drivers do not show any phenotype in the skin (Sahut-Barnola
26 et al. 2010; Dumontet et al. 2018). This is in agreement with the observation that lentiginos
27 usually appears very early (at birth or during childhood) in CNC patients independently from
28 endocrine manifestations (Stratakis 2016). Therefore, the skin phenotype of AdKO_{2.0} mice
29 should solely be the consequence of the recombinase activity of the *Sfl-Cre* driver. To evaluate
30 this hypothesis, we traced *Sfl-Cre* lineage in the skin by introducing the Cre recombinase
31 *mTmG* reporter transgene (Muzumdar et al. 2007) into WT and mutant mice. In compound
32
33
34
35
36
37
38
39
40
41
42
43
44
45
46
47
48
49
50
51
52
53
54
55
56
57
58
59
60

1
2
3 transgenic mice, Cre-mediated recombination fixes definitive eGFP expression in cells
4 expressing the *Sfl-Cre* transgene and in all their descending lineages. In abdominal skin
5 sections, eGFP immunostaining was limited to hair follicles (details in Figure S1d), while
6 strong eGFP expression was shown in the perigenital dermis of WT and AdKO mice (Figure
7 1c, bottom panels). Direct eGFP fluorescence was detected in specific areas of the skin of late
8 embryos, around the eyes, on the genitals, tail and the joint of the upper limbs (Figure S1c).
9
10 This demonstrates that the skin areas where postnatal pigmentation occurs in the case of
11 *Prkar1a* mutation, have been programmed during embryonic development and consist of
12 specific cell lineages currently expressing or having expressed the *Sfl-Cre* transgene early. This
13 enrichment of eGFP expression in pigmentation-prone skin areas was confirmed at the mRNA
14 level by RT-qPCR analyses in 5-day-old WT and mutant mice (Figure 1d). Although
15 steroidogenic activity of skin has been well documented (Slominski et al. 2013; Ceruti et al.
16 2018), SF-1 expression has been reported in only one study (Patel et al. 2001). Because we
17 never detected parallel induction nor significant expression of *Sf-1* in skin samples either using
18 RT-qPCR or immunostaining (not shown), skin eGFP-positive cells derived from *Sf-1* lineage
19 that no longer express *Sf-1*. As expected, we showed that in AdKO_{2.0} perigenital skin, *Prkar1a*
20 mRNA levels were decreased while transcripts for genes involved in melanosome biogenesis
21 (*Mlana/Mart1*) and melanogenesis (*Tryp-1* and *Tryp-2*) were increased compared to WT
22 (Figure S1e). Surprisingly, no change in mRNA levels was observed for genes encoding
23 melanogenic transcription factors (*Mitf*, *Sox9*, *Sox10*) or dermal fibroblastic markers (*Vimentin*
24 and *Colla1*) (Figure S1e).

25
26
27
28
29
30
31
32
33
34
35
36
37
38
39
40
41
42
43
44
45
46
47
48
49
50
51
52
53
54
55
56
57
58
59
60
The lack of variation in *Mitf* expression (a major melanocyte marker and regulator of genes
involved in melanogenesis) despite the marked increase in melanogenesis, has previously been
described in transgenic mouse models with dermal hyperpigmentation (Wolnicka-Glubisz et al.
2013). In addition, the unaltered expression of *Mitf* in AdKO_{2.0} perigenital skin samples, was

1
2
3 consistent with the unaltered expression of its positive upstream regulators, *Sox9* and *Sox10*
4 (Figure 1e) (Verastegui et al. 2000; Passeron et al. 2007). Altogether these results show a direct
5 correlation between location of lentigines in AdKO_{2.0} mice and *Sfl-Cre* activity in the dermis.
6
7
8
9
10 *Prkar1a* inactivation in these lentigines-prone areas is expected to increase PKA activity, which
11 in turn will enhance melanogenic activity of dermal melanocytes.
12
13

14
15 **Dermal *Sfl-Cre* lineages of the lentigines-prone areas are not melanocytes.** To identify the
16 dermal cells of the *Sfl-Cre* lineage, we carried out double immunohistochemical (IHC) analyses
17 using on the one hand, eGFP immunostaining which marks *Prkar1a*-negative recombined cells
18 and on the other hand, MLAN-A or VIMENTIN staining for melanocyte and fibroblast
19 immunodetection, respectively (Figure 2a-b). In the lentigines from AdKO_{2.0} mice, there was
20 no colocalization of eGFP and MLAN-A staining although eGFP cells were in close vicinity of
21 MLAN-A-positive cells. In contrast, eGFP-positive cells were all positive for vimentin,
22 indicating that *Prkar1a* invalidation occurred in dermal fibroblasts but not in dermal
23 melanocytes.
24
25
26
27
28
29
30
31
32
33
34
35

36 Fibroblasts play an important role in regulating the activities of melanocytes by secreting a
37 number of paracrine factors which bind to their receptors and modulate the intracellular
38 signaling cascades linked to melanocytic functions (Wang et al. 2017). We focused on three of
39 them and their corresponding receptors expressed on melanocytes, well characterized for their
40 pro-melanogenic actions: hepatocyte growth factor (HGF) and MET receptor (Matsumoto et al.
41 1991; Kunisada et al. 2000; Kapoor et al. 2020), endothelin 3 (EDN-3) and endothelin receptor
42 B (EDNRB) (Hosoda et al. 1994; Baynash et al. 1994; Bondurand et al. 2018) and Kit ligand
43 (KITL) and C-KIT receptor (Geissler et al. 1988; Copeland et al. 1990; Kasamatsu et al. 2008).
44
45 QPCR analyses showed an increase in mRNA levels of *Hgf* and *Edn3* and for their cognate
46 receptors *Met* and *Ednrb*, in AdKO_{2.0} lentigines (Figure 2c). These data are consistent with
47
48
49
50
51
52
53
54
55
56
57
58
59
60 previous observations from transgenic mice overexpressing HGF or EDN3 in the epidermis

1
2
3 which displayed skin hyperpigmentation associated with an increase of dermal melanocytes
4
5 (Kunisada et al. 2000; Aoki et al. 2009; Wolnicka-Glubisz et al. 2013). The mitogenic effect of
6
7 HGF has also been described in primary cultures of human melanocytes (Matsumoto et al.
8
9 1991). Under physiological condition, HGF production seemed to be linked to the pigmentation
10
11 of certain skin regions. Indeed, areas of the mouse skin with little hair, such as tail, nose, ear
12
13 and genitalia, were shown to contain far more dermal melanocytes than hairy regions and this
14
15 was associated, at least in part, with increased expression of HGF (Kunisada et al. 2000).
16
17

18
19 Our results also showed increased mRNA expression of *Edn3* and its receptor *Ebnrb*. These
20
21 were in agreement with data showing that *Edn3* overexpression from E13.5, induced an
22
23 increased proliferation of melanoblasts resulting in the presence of numerous dermal
24
25 melanocytes and dark skin at birth (Garcia et al. 2008). Similar mechanisms involving factors
26
27 identified in our animal model could also be relevant in humans. Indeed, mutations in either
28
29 *EDN3* or *EDNRB* genes have been associated with diminished pigmentation in patients with
30
31 Waardenburg syndrome (Mccallion and Chakravarti 2001). Furthermore, in patients with
32
33 neurofibromatosis type 1, skin hyperpigmentation was associated with increased production of
34
35 HGF by dermal fibroblasts (Okazaki et al. 2003).
36
37

38
39 In contrast, the mRNA encoding KITL and its receptor were not deregulated (Figure 2c).
40
41 Interestingly, mouse models that overexpressed HGF or EDN3 in the skin under the control of
42
43 the human *KRT14* promoter, displayed hyperpigmentation that was not influenced by KITL.
44
45 Indeed, blocking KITL signaling in these mice, by using either antibodies or a genetic approach,
46
47 did not affect skin hyperpigmentation while it completely inhibited that of the coat. These
48
49 previous findings and our present AdKO_{2.0} model provide independent and converging
50
51 arguments establishing a clear distinction between maintenance of dermal (and non-cutaneous)
52
53 melanocytes and epidermal melanocytes (contributing to hair pigmentation), based on their
54
55 differential requirement toward KIT signaling (Kunisada et al. 2000; Aoki et al. 2009).
56
57
58
59
60

1
2
3 In summary, the invalidation of *Prkar1a* in a subset of dermal fibroblasts (descending from a
4 cell lineage that has activated *Sfl-Cre*) induces the expression of the pro-melanogenic factors,
5
6 EDN3 and HGF, which in turn, increases the number of dermal melanocytes and/or stimulates
7
8 melanogenesis in lentigines-prone areas (Model in Figure 2d). Consistent with this result, HGF
9
10 is a known target of the cAMP-PKA pathway in human fibroblasts (Matsunaga et al. 1994).
11
12

13
14
15 **Dermal *Sfl-Cre* lineages induce nevi formation and promote the occurrence of cutaneous**

16 **myxomas in AdKO_{2.0} mice.** As early as 2 months of age, all AdKO_{2.0} mice developed nevi
17
18 symmetrically located on the posterior aspect of the thighs. These appeared deeply embedded
19
20 in the dermis and took on a blue color (Figure 3a). Histological staining and eGFP
21
22 immunostaining of blue nevi sections showed that melanin pigment deposits were found in the
23
24 vicinity of dermal cells that had lost *Prkar1a* conditional allele (eGFP positive) (Figure 3b).
25
26 Note that clusters of sebaceous glands (positive for cytokeratin 7, not shown), formed of eGFP-
27
28 negative cells with large cytoplasm, were also detected close to these pigmented formations.
29
30 Double immunostaining for eGFP/MLAN-A and eGFP/VIMENTIN confirmed that *Prkar1a*-
31
32 KO cells were fibroblasts (VIMENTIN positive) but not melanocytes (MLAN-A negative)
33
34 (Figure S2a). As expected, qPCR analyses of nevi formed in AdKO_{2.0} mice, showed an
35
36 increased expression of genes involved in melanogenesis (*Mlan-A*, *Tyrp-1* and *Tyrp-2*) and of
37
38 fibroblastic pro-melanogenic factors (*Hgf* and *Edn3*)(Figure S2b). The association between
39
40 HGF and MLAN-A protein accumulation was further confirmed in western blots (Figure 3c).
41
42 This increase in local HGF should also promote the differentiation of sebaceous glands in the
43
44 nevus area, which have been shown to express high levels of MET receptor (Zouboulis 2009;
45
46 Wu et al. 2014). Our results indicate that as with lentigines described above, blue nevi formation
47
48 in AdKO_{2.0} mice arises from activation of a pro-melanogenic fibroblast population, following
49
50 *Prkar1a* loss (Figure 2d and see Figure 4a for a summary diagram of pigmented skin areas in
51
52 AdKO_{2.0} mice).
53
54
55
56
57
58
59
60

1
2
3 In 20-50% of CNC patients, cutaneous myxomas were found localized in specific areas such as
4 the eyelid, external ear canal, areola and genitals (Correa et al. 2015; Espiard et al. 2020). About
5
6 44% of AdKO_{2.0} mice from 6 months of age, developed large skin tumors localized either on
7
8 the thighs or on the shoulder joint (where nevi occur) (Figure 4b). The tumor masses always
9
10 appeared dense, poorly vascularized, non-melanin and encapsulated. Hematoxylin staining
11
12 showed an epidermal delineation of the tumor (Figure 4c). CNC skin myxomas are composed
13
14 of spindle-shape cells and polygonal cells (Hachisuka et al. 2006). Similar histological features
15
16 were also observed in skin tumor masses of AdKO_{2.0} mice. The eGFP-labeled cells (*Prkar1a*-
17
18 KO cells) were found scattered throughout the entire tumor and accounted for at least 10% of
19
20 the total cell population, which consisted mainly of mesenchymal cells (vimentin positive),
21
22 indicating the myxomatous nature of these cutaneous tumors (Figure 4d). QPCR analyses
23
24 suggested that formation of skin myxomas could involve the dramatic increase (x100) in *Hgf*
25
26 gene expression while, as expected, *Edn-3* mRNA levels were not increased in these
27
28 nonpigmented lesions compared to blue nevi (Figure 4e). In conclusion, AdKO_{2.0} mice develop
29
30 cutaneous tumors that are hallmarks of skin lesions found in CNC patients. The occurrence of
31
32 myxomas in sites where blue nevi initially develop, suggests a possible continuity between
33
34 these pigmented lesions and myxoma formation.
35
36
37
38
39
40
41
42
43

44 **Lentigines and blue nevi from CNC patients.** With access to some rare skin samples from
45
46 CNC patients, we characterized the sites of melanin accumulation using Fontana Masson or
47
48 hematoxylin staining (Figure 5a, top; Figure S3a, top). Lentigines (Car-lentigo-1, Car-lentigo-
49
50 2) showed high levels of melanin pigments in the basal layer of the epidermis as previously
51
52 described (Courcoutsakis et al. 2013), while the pigmentation in blue nevi (Car-blue nevus-3,
53
54 Car-blue nevus-4) was rather concentrated in the dermis. In normal skin and lentigines, HGF
55
56 immunostaining was present in the epidermis and in scattered cells in the dermis, in agreement
57
58 with the literature showing HGF production in keratinocytes and fibroblasts (Serre et al. 2018).
59
60

1
2
3 In contrast, in blue nevi, HGF labeling was strong in the dermis (Figure 5a, bottom; Figure S3a,
4
5 bottom). Western blot analyses confirmed that HGF contents were high in pigmented skin
6
7 lesions from CNC patients that expressed high levels of the melanosome biogenesis marker
8
9 MLAN-A (Figure 5b).

10
11
12 HGF/VIMENTIN and HGF/MLAN-A double immunostaining was performed in blue nevi
13
14 sections (Figure 5c, similar results for Car-blue nevus-4, not shown). These experiments
15
16 showed co-localization of HGF staining with most of the numerous dermal fibroblasts
17
18 (VIMENTIN-positive). Using HGF/MLAN-A co-staining, two cell types could be identified:
19
20 1) strongly HGF-positive/MLAN-A-negative cells that should be HGF producing fibroblasts,
21
22 and 2) double positive cells that should be dermal melanocytes, on which HGF binds to enhance
23
24 melanogenesis.
25
26

27
28 We then interrogated the expression pattern of *PRKARIA* in CNC skin samples. As expected,
29
30 in CNC adrenal gland, R1 α immunostaining was only detected in internodular cortex where
31
32 *PRKARIA* is expressed from the intact allele and absent from nodules due to loss of
33
34 heterozygosity (Figure S3c). In normal skin or CNC lentigines, R1 α staining was detected in
35
36 both the dermis and in epidermal melanocytes (MLAN-A positive cells) (Figure S3b, bottom
37
38 right). In blue nevi, R1 α staining was present in most dermal cells, with the exception of a few
39
40 clusters of fibroblasts that strongly expressed HGF, presumably due to increased PKA activity
41
42 (Figure 5d). The lentigines formation in CNC patients did not appear associated with an
43
44 increase in HGF (Figure 5a, Figure S3a). This discrepancy with the AdKO_{2.0} model could rely
45
46 on species specificity, because unlike humans, the adult mouse epidermis lacks melanocytes
47
48 and, therefore, skin pigmentation solely relies on dermal melanocytes.
49
50
51
52
53

54
55 In conclusion, our results strongly argue that loss of R1 α in some dermal fibroblasts induces
56
57 PKA-dependent production of secreted growth factors including HGF, which in turn, stimulate
58
59 melanogenic activity of dermal melanocytes. This non-cell-autonomous mechanism of
60

1
2
3 *PRKARIA*-dependent blue nevus pathogenesis in CNC patients is consistent with what we
4
5 demonstrated in the skin lesions of AdKO_{2.0} mice, which ultimately might evolve into massive
6
7 skin myxomas (Figure 2d). There is great heterogeneity in the origin, location and functions of
8
9 skin fibroblasts. For example, cell fate mapping analyses performed on the avian or mouse
10
11 embryo revealed that skin fibroblasts of the dorsal, ventral, lateral or craniofacial dermis are
12
13 derived from different embryonic tissues (Thulabandu et al. 2018). Our cell lineage tracing
14
15 experiments in mice suggest that the pigmented skin lesions typical of CNC, form through the
16
17 *Prkar1a*-dependent activation of a specific subpopulation of dermal fibroblasts sharing
18
19 common origin with the steroidogenic lineage. Most recent studies investigating the lineage
20
21 diversity of fibroblast populations have focused primarily on the mechanisms of hair follicle
22
23 formation and repair (Driskell et al. 2013; Joost et al. 2020). Therefore, we hypothesize that the
24
25 specific distribution of cutaneous pigmented lesions in CNC may rely on the paracrine activity
26
27 of specific dermal fibroblast populations, preferentially located in areas enriched in dermal
28
29 melanocytes, sharing possible common origins with SF-1 lineage and having increased
30
31 sensitivity to changes in PKA activity.
32
33
34
35
36
37
38
39

40 **MATERIALS & METHODS**

41
42
43 **Mouse.** The *Prkar1a*^{fl/fl}::*Sf1*^{cre/+}::*R26R*^{mTmG/+} mouse line have been described previously
44
45 ((Muzumdar et al. 2007; Drelon et al. 2016). Mice were all maintained and bred on a mixed
46
47 background. Throughout, WT refers *Prkar1a*^{fl/+}::*Sf1*^{cre/+}::*R26R*^{mTmG/+} in which we did not
48
49 observe any discernible phenotype. Littermate control animals were used in all experiments.
50
51
52

53 **Histology and immunostaining.** For general morphology and melanin detection, sections were
54
55 stained with hematoxylin and eosin and with Fontana Masson staining (MF-100-T ; Biognost),
56
57 following the manufacturer's instructions. Immunohistological methods have been previously
58
59
60

1
2
3 described (Drelon et al. 2016). Cell count was performed using the QuPath software (Bankhead
4
5 et al. 2017). See Table S1 for conditions used.
6
7

8
9 **Western blot.** Twenty five (mouse WB) or twelve (human WB) micrograms of total proteins
10
11 were loaded on 4/15% SDS-page gel, transfer on nitrocellulose and detected with primary
12
13 antibodies (Table S1). Signals were quantified with ChemiDoc MP Imaging System camera
14
15 system (Bio-rad) and Image Lab software (Bio-rad). Expression of proteins were normalized to
16
17 expression of the ACTIN or GAPDH protein.
18
19

20
21 **Real-time PCR analysis.** Total RNAs were extracted from skin using the RNeasy nucleotide
22
23 extraction kit (Macherey Nagel), following the manufacturer's instructions. One microgram of
24
25 total mRNAs was reverse transcribed for 1h at 37C with 5pmol of random hexamers primers,
26
27 200 units reverse transcriptase (M-MLV RT, M1701, Promega), 2mM dNTPs and 20 units
28
29 RNAsin (N2615, Promega). One microlitre of a one-fourth dilution of cDNA was used in each
30
31 qPCR. PCR reactions were conducted with SYBR qPCR Premix Ex Taq II Tli RNaseH+
32
33 (TAKRR820W, Takara). Primer pairs are listed in Table S2. For each experiment and primer
34
35 pairs, efficiency of PCR reactions was evaluated by amplification of serial dilutions of a mix of
36
37 cDNAs. Relative gene expression was obtained by the DDCT method after normalization to
38
39 actin.
40
41
42
43

44
45 **Samples from patients.** Histological slides of skin lesions from CNC patients and skin biopsies
46
47 were obtained from Pr C.A. Stratakis lab, NIH. Human adult normal skin sections were used as
48
49 control for histological analyses (UM-HuFPT136, CliniSciences). Sample information are
50
51 available in Tables S3 & S4.
52
53

54
55 **Statistics.** Statistical analyses were conducted by Man Whitney test. P values of less than 0.05
56
57 were considered significant. All the data are represented by Box & Whiskers Plots with the
58
59 minimum and maximum value and the median.
60

1
2
3 **Study Approval.** All animal studies were approved by Ethics Committee for Animal
4
5
6
7
8
9
10
11
12
13
14
15
16
17
18
19
20
21
22
23
24
25
26
27
28
29
30
31
32
33
34
35
36
37
38
39
40
41
42
43
44
45
46
47
48
49
50
51
52
53
54
55
56
57
58
59
60

Experimentation in Auvergne (N° 21153-2019061912044646V2) and were conducted in agreement with international standards for animal welfare.

All patients gave informed consent for the use of their resected tissues for research purposes.

ORCiDs

Isabelle SAHUT-BARNOLA : <https://orcid.org/0000-0001-7004-8577>

A-Marie LEFRANCOIS-MARTINEZ : <https://orcid.org/0000-0003-2021-2548>

Damien DUFOUR : <https://orcid.org/0000-0002-1220-1745>

Jean-Marie BOTTO : <https://orcid.org/0000-0002-6182-4236>

Crystal KAMILARIS : <https://orcid.org/0000-0002-3872-0447>

Fabio R. FAUCZ : <https://orcid.org/0000-0001-7959-9842>

Constantine A. STRATAKIS : <https://orcid.org/0000-0002-4058-5520>

Pierre VAL : <https://orcid.org/0000-0001-7648-5567>

Antoine MARTINEZ : <https://orcid.org/0000-0001-9304-5061>

CONFLICT OF INTEREST

The authors have declared that no conflict of interest exists

ACKNOWLEDGMENTS

1
2
3
4
5
6
7
8
9
10
11
12
13
14
15
16
17
18
19
20
21
22
23
24
25
26
27
28
29
30
31
32
33
34
35
36
37
38
39
40
41
42
43
44
45
46
47
48
49
50
51
52
53
54
55
56
57
58
59
60

This work was funded through institutional support from Centre National de la Recherche Scientifique, INSERM, Université Clermont-Auvergne and by Agence Nationale pour la Recherche (ANR-18-CE14-0012-02).

AUTHORS CONTRIBUTIONS

ISB, AMLM, DD, JMB and AM designed experiments. ISB, AMLM, PV and AM prepared manuscript. ISB and AM supervised the project. CK, FRF and CAS provided human samples and clinical information. All authors edited the manuscript.

For Review Only

REFERENCES

- Amaya JM, Suidgeest E, Sahut-Barnola I, Dumontet T, Montanier N, Pagès G, et al. Effects of Long-Term Endogenous Corticosteroid Exposure on Brain Volume and Glial Cells in the AdKO Mouse. *Front Neurosci* [Internet]. 2021 Feb 10 [cited 2021 May 21];15:604103. Available from: <https://www.frontiersin.org/articles/10.3389/fnins.2021.604103/full>
- Aoki H, Yamada Y, Hara A, Kunisada T. Two distinct types of mouse melanocyte: differential signaling requirement for the maintenance of non-cutaneous and dermal versus epidermal melanocytes. *Development* [Internet]. 2009 Aug 1 [cited 2020 Apr 30];136(15):2511–21. Available from: <http://dev.biologists.org/cgi/doi/10.1242/dev.037168>
- Bankhead P, Loughrey MB, Fernández JA, Dombrowski Y, McArt DG, Dunne PD, et al. QuPath: Open source software for digital pathology image analysis. *Sci Rep*. 2017 Dec 4;7(1):16878.
- Baynash AG, Hosoda K, Giaid A, Richardson JA, Emoto N, Hammer RE, et al. Interaction of endothelin-3 with endothelin-B receptor is essential for development of epidermal melanocytes and enteric neurons. *Cell*. 1994 Dec 30;79(7):1277–85.
- Bingham NC, Verma-Kurvari S, Parada LF, Parker KL. Development of a steroidogenic factor 1/Cre transgenic mouse line. *genesis*. 2006 Sep;44(9):419–24.
- Bondurand N, Dufour S, Pingault V. News from the endothelin-3/EDNRB signaling pathway: Role during enteric nervous system development and involvement in neural crest-associated disorders. *Developmental Biology* [Internet]. 2018 Dec [cited 2020 Apr 29];444:S156–69. Available from: <https://linkinghub.elsevier.com/retrieve/pii/S001216061830441X>
- Carney JA, Gordon H, Carpenter PC, Shenoy BV, Go VL. The complex of myxomas, spotty pigmentation, and endocrine overactivity. *Medicine (Baltimore)*. 1985 Jul;64(4):270–83.
- Casey M, Vaughan CJ, He J, Hatcher CJ, Winter JM, Weremowicz S, et al. Mutations in the protein kinase A R1 α regulatory subunit cause familial cardiac myxomas and Carney complex. *J Clin Invest* [Internet]. 2000 Sep 1 [cited 2020 May 7];106(5):R31–8. Available from: <http://www.jci.org/articles/view/10841>
- Ceruti JM, Leirós GJ, Balaña ME. Androgens and androgen receptor action in skin and hair follicles. *Mol Cell Endocrinol*. 2018 Apr 15;465:122–33.
- Copeland NG, Gilbert DJ, Cho BC, Donovan PJ, Jenkins NA, Cosman D, et al. Mast cell growth factor maps near the steel locus on mouse chromosome 110 and is deleted in a number of steel alleles. *Cell* [Internet]. 1990 Oct [cited 2020 Apr 29];63(1):175–83. Available from: <https://linkinghub.elsevier.com/retrieve/pii/009286749090298S>
- Correa R, Salpea P, Stratakis CA. Carney complex: an update. *European Journal of Endocrinology* [Internet]. 2015 Oct [cited 2020 May 4];173(4):M85–97. Available from: <https://aje.bioscientifica.com/view/journals/eje/173/4/M85.xml>

- 1
2
3 Courcoutsakis NA, Tatsi C, Patronas NJ, Lee C-CR, Prassopoulos PK, Stratakis CA. The
4 complex of myxomas, spotty skin pigmentation and endocrine overactivity (Carney
5 complex): imaging findings with clinical and pathological correlation. *Insights*
6 *Imaging* [Internet]. 2013 Feb [cited 2021 Apr 28];4(1):119–33. Available from:
7 <http://link.springer.com/10.1007/s13244-012-0208-6>
8
9
10 Drelon C, Berthon A, Sahut-Barnola I, Mathieu M, Dumontet T, Rodriguez S, et al. PKA
11 inhibits WNT signalling in adrenal cortex zonation and prevents malignant tumour
12 development. *Nat Commun* [Internet]. 2016 Nov [cited 2020 Apr 27];7(1):12751.
13 Available from: <http://www.nature.com/articles/ncomms12751>
14
15 Driskell RR, Lichtenberger BM, Hoste E, Kretzschmar K, Simons BD, Charalambous M, et
16 al. Distinct fibroblast lineages determine dermal architecture in skin development and
17 repair. *Nature* [Internet]. 2013 Dec [cited 2021 Apr 28];504(7479):277–81. Available
18 from: <http://www.nature.com/articles/nature12783>
19
20
21 Dumontet T, Sahut-Barnola I, Septier A, Montanier N, Plotton I, Roucher-Boulez F, et al.
22 PKA signaling drives reticularis differentiation and sexually dimorphic adrenal cortex
23 renewal. *JCI Insight* [Internet]. 2018 Jan 25 [cited 2020 May 7];3(2):e98394.
24 Available from: <https://insight.jci.org/articles/view/98394>
25
26
27 Espiard S, Vantyghem M-C, Assié G, Cardot-Bauters C, Raverot G, Brucker-Davis F, et al.
28 Frequency and Incidence of Carney Complex Manifestations: A Prospective
29 Multicenter Study With a Three-Year Follow-Up. *J Clin Endocrinol Metab*. 2020 Mar
30 1;105(3).
31
32
33 Garcia RJ, Ittah A, Mirabal S, Figueroa J, Lopez L, Glick AB, et al. Endothelin 3 Induces
34 Skin Pigmentation in a Keratin-Driven Inducible Mouse Model. *Journal of*
35 *Investigative Dermatology* [Internet]. 2008 Jan [cited 2021 Apr 16];128(1):131–42.
36 Available from: <https://linkinghub.elsevier.com/retrieve/pii/S0022202X15336022>
37
38
39 Geissler EN, Ryan MA, Housman DE. The dominant-white spotting (W) locus of the mouse
40 encodes the c-kit proto-oncogene. *Cell*. 1988 Oct 7;55(1):185–92.
41
42
43 Hachisuka J, Ichikawa M, Moroi Y, Urabe K, Furue M. A case of Carney complex. *Int J*
44 *Dermatol* [Internet]. 2006 Dec [cited 2021 May 27];45(12):1406–7. Available from:
45 <http://doi.wiley.com/10.1111/j.1365-4632.2006.02889.x>
46
47
48 Hosoda K, Hammer RE, Richardson JA, Baynash AG, Cheung JC, Giaid A, et al. Targeted
49 and natural (piebald-lethal) mutations of endothelin-B receptor gene produce
50 megacolon associated with spotted coat color in mice. *Cell*. 1994 Dec 30;79(7):1267–
51 76.
52
53
54 Joost S, Annusver K, Jacob T, Sun X, Dalessandri T, Sivan U, et al. The Molecular Anatomy
55 of Mouse Skin during Hair Growth and Rest. *Cell Stem Cell* [Internet]. 2020 Mar
56 [cited 2021 Apr 28];26(3):441-457.e7. Available from:
57 <https://linkinghub.elsevier.com/retrieve/pii/S1934590920300126>
58
59
60 Kapoor R, Dhatwalia SK, Kumar R, Rani S, Parsad D. Emerging Role of Dermal
61 Compartment in Skin Pigmentation: Comprehensive Review. *J Eur Acad Dermatol*
62 *Venereol* [Internet]. 2020 Apr 3 [cited 2020 Apr 29]; Available from:
63 <http://doi.wiley.com/10.1111/jdv.16404>

- 1
2
3 Kasamatsu S, Hachiya A, Higuchi K, Ohuchi A, Kitahara T, Boissy RE. Production of the
4 Soluble Form of KIT, s-KIT, Abolishes Stem Cell Factor-Induced Melanogenesis in
5 Human Melanocytes. *Journal of Investigative Dermatology* [Internet]. 2008 Jul [cited
6 2020 Apr 29];128(7):1763–72. Available from:
7 <https://linkinghub.elsevier.com/retrieve/pii/S0022202X15339427>
8
9
10 Kirschner LS, Carney JA, Pack SD, Taymans SE, Giatzakis C, Cho YS, et al. Mutations of
11 the gene encoding the protein kinase A type I- α regulatory subunit in patients with the
12 Carney complex. *Nat Genet* [Internet]. 2000 Sep [cited 2020 May 6];26(1):89–92.
13 Available from: http://www.nature.com/articles/ng0900_89
14
15
16 Kunisada T, Yamazaki H, Hirobe T, Kamei S, Omoteno M, Tagaya H, et al. Keratinocyte
17 expression of transgenic hepatocyte growth factor affects melanocyte development,
18 leading to dermal melanocytosis. *Mechanisms of Development* [Internet]. 2000 Jun
19 [cited 2020 Apr 29];94(1–2):67–78. Available from:
20 <https://linkinghub.elsevier.com/retrieve/pii/S0925477300003087>
21
22
23 Matsumoto K, Tajima H, Nakamura T. Hepatocyte growth factor is a potent stimulator of
24 human melanocyte DNA synthesis and growth. *Biochemical and Biophysical
25 Research Communications* [Internet]. 1991 Apr [cited 2020 Apr 29];176(1):45–51.
26 Available from: <https://linkinghub.elsevier.com/retrieve/pii/0006291X9190887D>
27
28 Matsunaga T, Gohda E, Takebe T, Wu YL, Iwao M, Kataoka H, et al. Expression of
29 hepatocyte growth factor is up-regulated through activation of a cAMP-mediated
30 pathway. *Exp Cell Res*. 1994 Feb;210(2):326–35.
31
32
33 Mccallion AS, Chakravarti A. *EDNRB/EDN3* and Hirschsprung Disease Type II:
34 *EDNRB/EDN3* and Hirschsprung Disease Type II. *Pigment Cell Research* [Internet].
35 2001 Jun [cited 2021 Apr 16];14(3):161–9. Available from:
36 <http://doi.wiley.com/10.1034/j.1600-0749.2001.140305.x>
37
38 Muzumdar MD, Tasic B, Miyamichi K, Li L, Luo L. A global double-fluorescent Cre reporter
39 mouse. *genesis* [Internet]. 2007 Sep [cited 2020 Apr 27];45(9):593–605. Available
40 from: <http://doi.wiley.com/10.1002/dvg.20335>
41
42
43 Okazaki M, Yoshimura K, Suzuki Y, Uchida G, Kitano Y, Harii K, et al. The mechanism of
44 epidermal hyperpigmentation in café-au-lait macules of neurofibromatosis type 1 (von
45 Recklinghausen’s disease) may be associated with dermal fibroblast-derived stem cell
46 factor and hepatocyte growth factor. *Br J Dermatol*. 2003 Apr;148(4):689–97.
47
48
49 Passeron T, Valencia JC, Bertolotto C, Hoashi T, Le Pape E, Takahashi K, et al. SOX9 is a
50 key player in ultraviolet B-induced melanocyte differentiation and pigmentation.
51 *Proceedings of the National Academy of Sciences* [Internet]. 2007 Aug 28 [cited 2020
52 Apr 28];104(35):13984–9. Available from:
53 <http://www.pnas.org/cgi/doi/10.1073/pnas.0705117104>
54
55
56 Patel MV, McKay IA, Burrin JM. Transcriptional regulators of steroidogenesis, DAX-1 and
57 SF-1, are expressed in human skin. *J Invest Dermatol*. 2001 Dec;117(6):1559–65.
58
59
60 Sahut-Barnola I, de Jousineau C, Val P, Lambert-Langlais S, Damon C, Lefrançois-Martinez
A-M, et al. Cushing’s Syndrome and Fetal Features Resurgence in Adrenal Cortex–
Specific Prkar1a Knockout Mice. McKnight GS, editor. *PLoS Genet* [Internet]. 2010

- 1
2
3 Jun 10 [cited 2020 Apr 27];6(6):e1000980. Available from:
4 <https://dx.plos.org/10.1371/journal.pgen.1000980>
5
- 6 Serre C, Busuttill V, Botto J-M. Intrinsic and extrinsic regulation of human skin
7 melanogenesis and pigmentation. *Int J Cosmet Sci*. 2018 Aug;40(4):328–47.
8
- 9 Slominski A, Zbytek B, Nikolakis G, Manna PR, Skobowiat C, Zmijewski M, et al.
10 Steroidogenesis in the skin: Implications for local immune functions. *The Journal of*
11 *Steroid Biochemistry and Molecular Biology* [Internet]. 2013 Sep [cited 2021 May
12 27];137:107–23. Available from:
13 <https://linkinghub.elsevier.com/retrieve/pii/S0960076013000277>
14
- 15 Stratakis CA. Carney complex: A familial lentiginosis predisposing to a variety of tumors.
16 *Rev Endocr Metab Disord* [Internet]. 2016 Sep [cited 2020 May 5];17(3):367–71.
17 Available from: <http://link.springer.com/10.1007/s11154-016-9400-1>
18
- 19 Thulabandu V, Chen D, Atit RP. Dermal fibroblast in cutaneous development and healing.
20 *Wiley Interdiscip Rev Dev Biol*. 2018 Mar;7(2).
21
- 22 Verastegui C, Bille K, Ortonne J-P, Ballotti R. Regulation of the Microphthalmia-associated
23 Transcription Factor Gene by the Waardenburg Syndrome Type 4 Gene, *SOX10*. *J*
24 *Biol Chem* [Internet]. 2000 Oct 6 [cited 2020 Apr 28];275(40):30757–60. Available
25 from: <http://www.jbc.org/lookup/doi/10.1074/jbc.C000445200>
26
- 27 Wang Y, Viennet C, Robin S, Berthon J-Y, He L, Humbert P. Precise role of dermal
28 fibroblasts on melanocyte pigmentation. *Journal of Dermatological Science* [Internet].
29 2017 Nov [cited 2020 Apr 29];88(2):159–66. Available from:
30 <https://linkinghub.elsevier.com/retrieve/pii/S0923181117300828>
31
- 32 Wolnicka-Glubisz A, Pecio A, Podkowa D, Plonka PM, Grabacka M. HGF/SF Increases
33 Number of Skin Melanocytes but Does Not Alter Quality or Quantity of Follicular
34 Melanogenesis. Slominski AT, editor. *PLoS ONE* [Internet]. 2013 Nov 6 [cited 2020
35 Apr 28];8(11):e74883. Available from:
36 <http://dx.plos.org/10.1371/journal.pone.0074883>
37
- 38 Wu B-Y, Lee S-P, Hsiao H-C, Chiu H, Chen C-Y, Yeo YH, et al. Matriptase expression and
39 zymogen activation in human pilosebaceous unit. *J Histochem Cytochem*. 2014
40 Jan;62(1):50–9.
41
- 42 Zouboulis CC. Sebaceous gland receptors. *Dermatoendocrinol*. 2009 Mar;1(2):77–80.
43
- 44 The Coat Colors of Mice by Willys K. Silvers [Internet]. [cited 2021 May 27]. Available
45 from: <http://www.informatics.jax.org/wksilvers/index.shtml>
46
47
48
49
50
51
52
53
54
55
56
57
58
59
60

FIGURE LEGENDS

Figure 1: Skin pigmentation abnormalities in AdKO_{2.0} mice is associated with *Sfl-Cre* dermal activity. a-b. AdKO_{2.0} newborns (a, top) show pigmentation ring around the eye (arrows). At 5 days, pigmentation defects appear as black spots under the eye (arrows in a, bottom) and in specific locations (arrows in b, details in Figure S1). c. Fontana Masson (FM) staining (melanin) and eGFP immunodetection in WT (*Prkar1a^{fl/+}::Sfl-Cre/+::R26R^{mTmG/+}*) and AdKO_{2.0} (*Prkar1a^{fl/fl}::Sfl-Cre/+::R26R^{mTmG/+}*) (5-day-old) abdominal (top square in b) and perigenital (bottom square in b) skin sections. Hoechst nuclei staining (H). Scale bars=50µm. Epi: Epidermis, Der: Dermis. d. qPCR analysis of eGFP (proxy for recombination) in perigenital and/or areola skin compared to in WT and AdKO_{2.0} abdominal skin (5-day-old). *N*, indicated above graph. Statistical analyses: Mann Whitney test. ***P<0.001.

Figure 2: eGFP+ dermal cells (Prkar1a-KO) are PKA-reprogrammed fibroblasts producing melanogenic signals. a-b. eGFP (Prkar1a-KO cells) and MLAN-A (melanocytes) (a), or VIMENTIN (mesenchymal cells) (b) co-labelings, in AdKO_{2.0} perigenital skin (5-day-old). Hoechst nuclei staining (H). Insets, dotted frames magnification. Epi: Epidermis, Der: Dermis. Scale bars=20µm. c. qPCR analyses of WT/AdKO_{2.0} perigenital skin samples (5-day-old) for fibroblast secreted factors and corresponding receptors on melanocytes. *N*, indicated under graphs. Statistical analyses: Mann Whitney test. *P<0.05, **P<0.01, ***P<0.001. d. Schema representing skin effects of *Prkar1a/PRKARIA* loss (AdKO_{2.0} mice/CNC patients). Increased production of diffusible factors (HGF, EDN-3) in response to PKA activation in dermal fibroblasts descending from a cell lineage that has activated *Sfl-Cre*, is expected to increase number and melanogenic activity of dermal melanocytes, favoring lentiginos/nevi formation in prone areas.

1
2
3 **Figure 3: Increased PKA activity is associated with blue nevi in AdKO_{2.0} skin.** a. View of
4 symmetrical nevi (top) and magnification (bottom) in 4-6-month-old females. b. Hematoxylin
5 staining and eGFP immunodetection of blue nevus section from 6-month-old AdKO_{2.0} female.
6
7 In nevus section, the central cavity (CC) represents the place where melanin accumulates
8 (eliminated by histological treatments). The periphery of the cavity is lined by melanin
9 pigments, eGFP-positive cells and by clusters of sebaceous glands formed of eGFP-negative
10 cells with large cytoplasm (* in the magnification panels). Scale bars=100µm. c. Western blot
11 analyses of MLAN-A and HGF protein accumulation in skin extracts from WT and AdKO_{2.0}
12 (nevi) mice. Graphs showed quantification normalized to ACTIN signal. *N*, indicated under
13 graphs. Statistical analyses: Mann Whitney test. *P<0.05; **P<0.01.

14
15
16
17
18
19
20
21
22
23
24
25
26 **Figure 4: Cutaneous myxomas in AdKO_{2.0} mice.** a. Skin lesions maps in 5-day- and 2-month-
27 old mice. Head lentigines are no longer seen in adults due to hair growth. Nevi form
28 symmetrically on back of thighs and shoulders. b. Myxomas emerge in 44% of AdKO_{2.0} mice
29 (≥6 months), in areas where nevi form. Scale bar=1cm. c-d. The tumor is delimited by epidermis
30 (Epi). eGFP (c) or Vimentin (d) immunodetections (insets, frame magnification) and
31 hematoxylin counterstaining. Percentages of eGFP-positive (Prkar1a-KO) and Vimentin-
32 positive cells are calculated from counts of four different tumors. Scale bar=100µm. e. qPCR
33 analyses of fibroblastic secreted factors in WT skin (sampling located where nevi form in
34 mutants) and AdKO_{2.0} nevi (3-month-old females) and in AdKO_{2.0} myxomas. *N*, indicated under
35 graphs. Statistical analyses: Mann Whitney test. **P<0.01.

36
37
38
39
40
41
42
43
44
45
46
47
48
49
50 **Figure 5: Increased HGF is associated with dermal melanin in blue nevi from CNC**
51 **patients.** a. Fontana Masson (FM) staining and HGF immunodetection of normal human skin
52 and lentigines/blue nevi from CNC patients. b. Western blot analysis of MLAN-A and HGF
53 protein accumulation in skin extracts from CNC patients. c. Co-immunolabeling of HGF (green
54 arrows) and VIMENTIN (mesenchymal cells, red arrows) in top panels, or MLAN-A
55
56
57
58
59
60

1
2
3 (melanocytes, red arrows) in bottom panels in blue nevus from CNC patients (Striped arrows,
4 cells co-labelled with HGF and VIMENTIN/MLAN-A). d. Co-immunofluorescent labeling of
5 R1 α and HGF in blue nevus from CNC patients. Hoechst nuclei staining (H). Insets are
6 magnification of dotted frames. Epi: Epidermis, Der: Dermis. Scale bars=50 μ m.
7
8
9
10
11
12
13
14
15
16
17
18
19
20
21
22
23
24
25
26
27
28
29
30
31
32
33
34
35
36
37
38
39
40
41
42
43
44
45
46
47
48
49
50
51
52
53
54
55
56
57
58
59
60

For Review Only

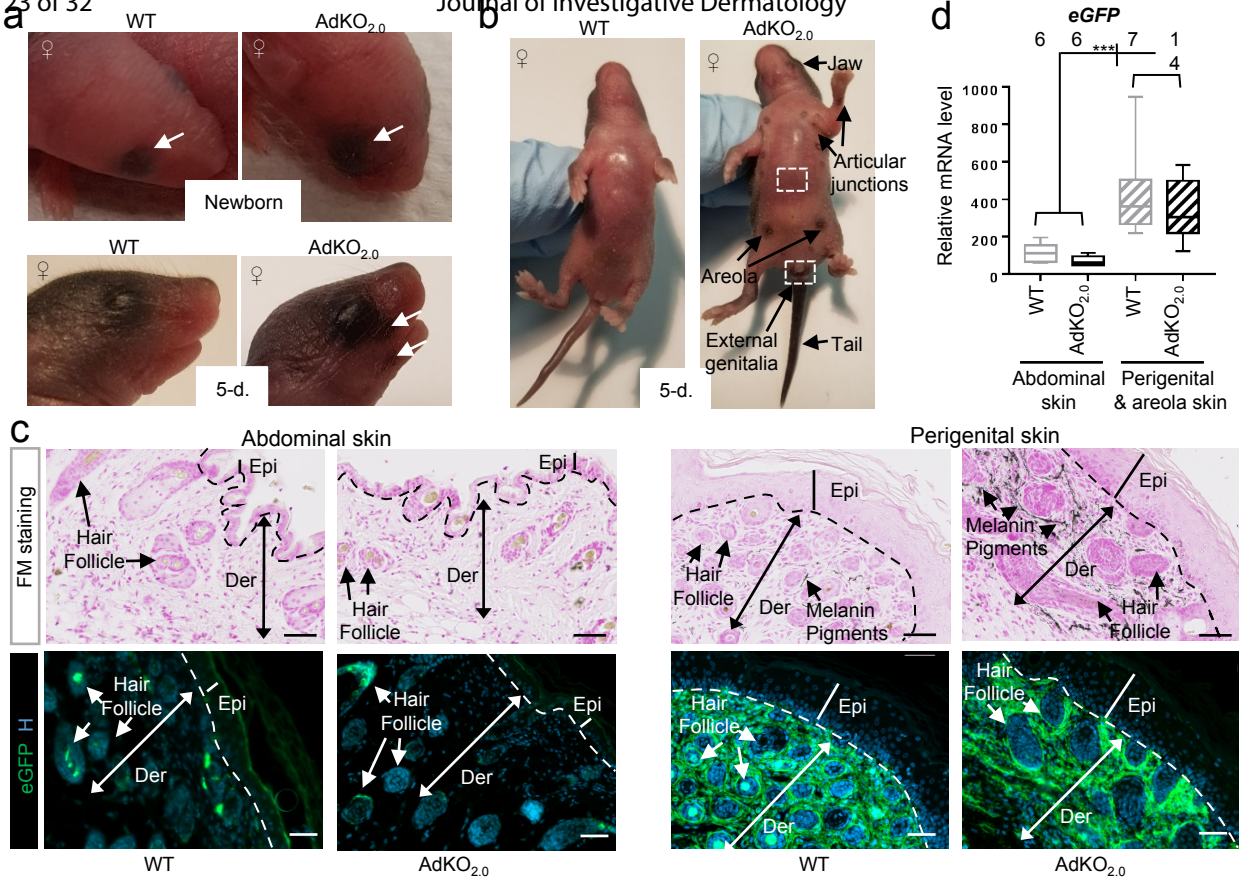


Figure 1

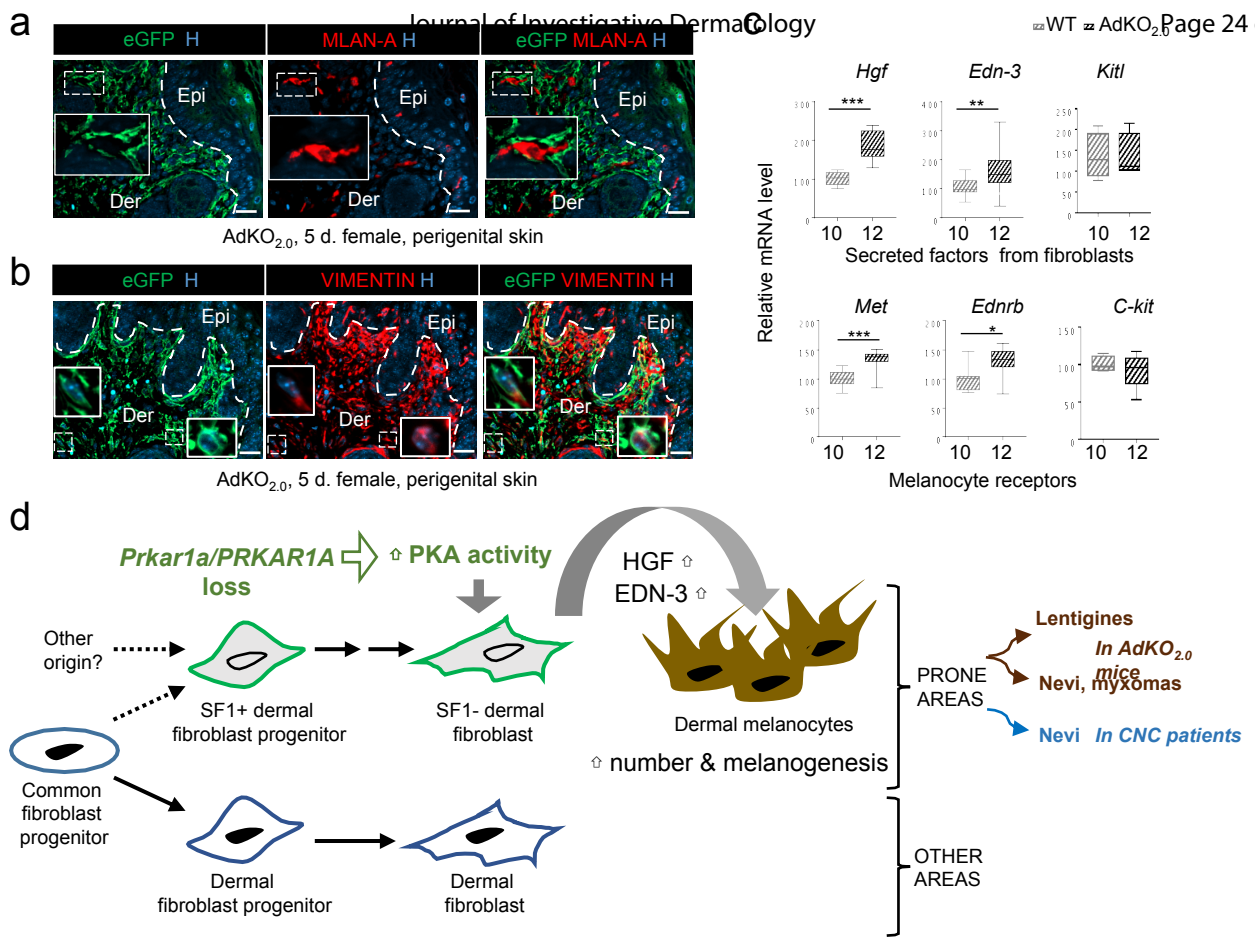


Figure
2

1
2
3
4
5
6
7
8
9
10
11
12
13
14
15
16
17
18
19
20
21
22
23
24
25
26
27
28
29
30
31
32
33
34
35
36
37
38
39
40
41
42
43
44
45
46
47
48
49
50
51
52
53
54
55
56

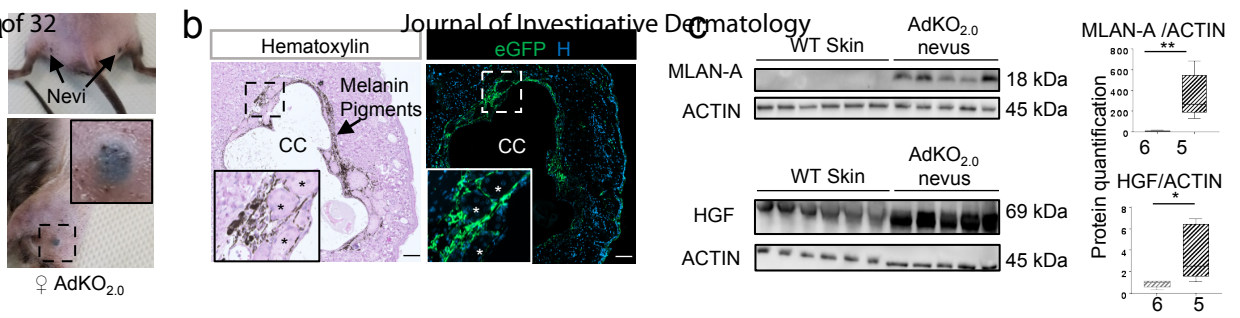


Figure 3

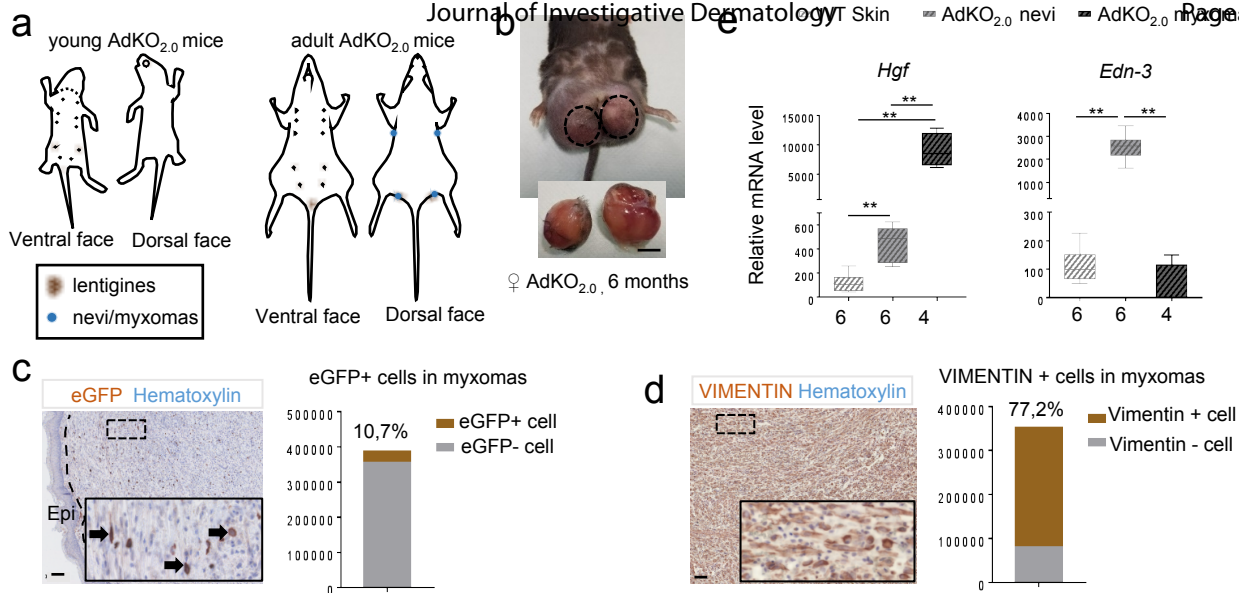
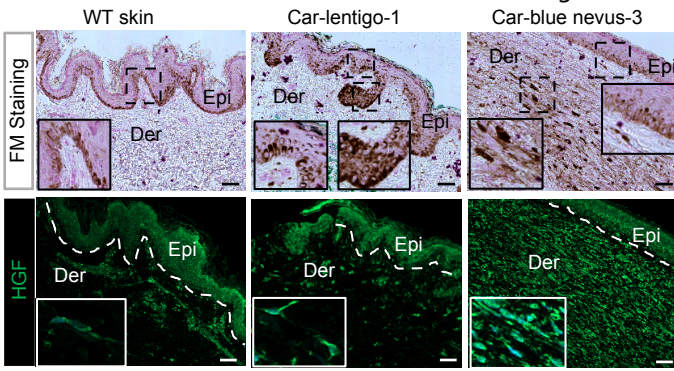
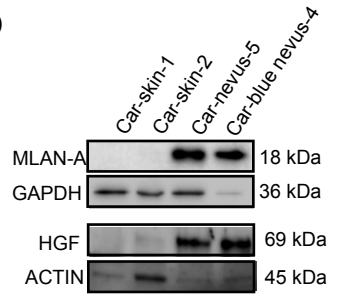


Figure 4

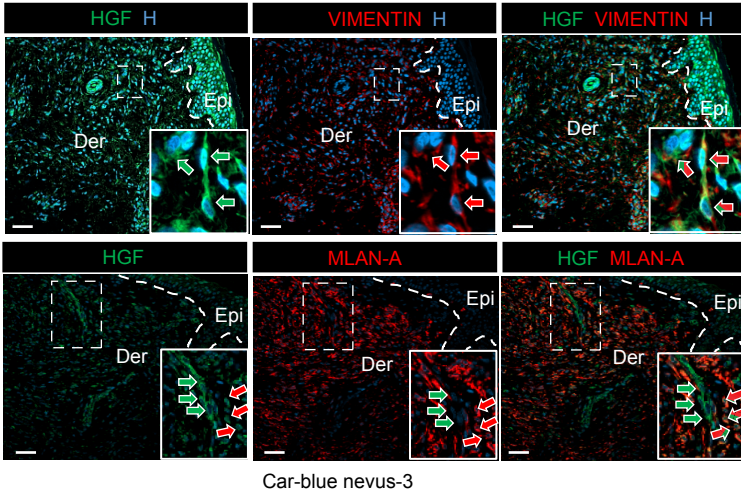
a



b



c



d

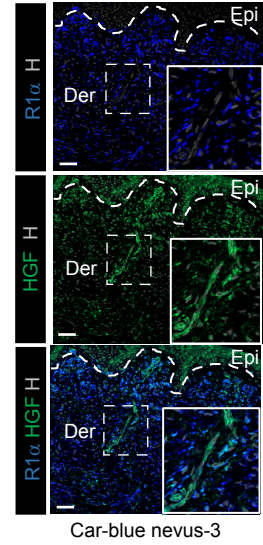


Figure 5

Table S1: Immunohistological and western blot conditions

Immunohistochemistry and immunofluorescence					
Antibody	Supplier	Reference	Host	dilution	Epitope retrieval
GFP	Invitrogen	A11122	Rabbit	1/1500	25 min. boiling in TE solution (Tris 10mM, EDTA1mM, pH9.0)
GFP	Abcam	5450	Goat	1/1000	
HGF	R&D systems	AB-294-NA	Goat	1/100	
MLANA	Abclonal	A6290	Rabbit	1/200	
PRKAR1A	BD biosciences	610610	Mouse	1/400	
VIMENTIN	Cell Signaling	5741	Rabbit	1/1000	

Western Blot					
Antibody	Supplier	Reference	Host	dilution	Blocking
ACTIN	Sigma	A2066	Rabbit	1/5000	Milk 10%
GAPDH	Sigma	G9545	Rabbit	1/10000	
HGF	R&D systems	AB-294-NA	Goat	1/250	
MLANA	Abclonal	A6290	Rabbit	1/1000	

Table S2: Sequences of the primers used for RTqPCR

Target	Forward (5'-3')	Reverse (5'-3')
<i>Actin</i>	TCATCACTATTGGCAACGAGC	AGTTTCATGGATGCCACAGG
<i>C-kit</i>	AGGTGTACCACTCCTGTCT	TCCTCGACAACCTTCCATTG
<i>Edn3</i>	GCTGCACGTGCTTCACTTAC	TTTCTGGAAGTGGCCCAAG
<i>Ednrb</i>	TCGCTCTGTATTTGGTGAGCA	ATTCGGCGAGTGTTCTTGC
<i>eGFP</i>	GAAGCAGCACGACTTCTTCAAG	AAGTCGATGCCCTTCAGCTC
<i>Hgf</i>	GGGACCCTGGTGTTCACAA	CATCAAAGCCCTTGTCGGGA
<i>Kitl</i>	ACGTCTGAGTGCTGAAAACCC	CACCATCCAGGCTGAAATCTAC
<i>Mlana</i>	GCACAGACGCTCCTATGTCA	AGTACCAGCAGCCGATAAGC
<i>Col1A1</i>	CGACCTCAAGATGTGCCACT	CCATCGGTCATGCTCTCTCC
<i>Met</i>	ACCCAAGGTACAAACTCCAG	AAGCGTTCTGCTACACCGTC
<i>Mitf</i>	CCAGGCCTTACCATCAGCAA	AGCTCCTTAATGCGGTCGTT
<i>Prkar1a</i>	CGGGAATGCGAGCTCTATGT	CTCGAGTCAGTACGGATGCC
<i>Sox10</i>	ATGTCAGATGGGAACCCAGA	GTCTTTGGGGTGGTTGGAG
<i>Sox9</i>	GCGGAGCTCAGCAAGACTCTG	ATCGGGGTGGTCTTTCTTGTG
<i>Tyrp1</i>	GGATTCATGGTACTGGTGAGCA	TGGAAACTGAGCCCAAACCT
<i>Tyrp2</i>	TAAGCAGTATGGCTGGAGCAC	CTTCTCGCCAGTCTTCCTTGT
<i>Vim</i>	GGATCAGCTCACCAACGACA	AAGGTCAAGACGTGCCAGAG

Table S3: Human skin Information

Number	Identification Number	Diagnosis	Sample
Car-skin-1	CAR 27.04	Skin myxoma	Sample for WB
Car-skin-2	CMC.01	Spitz nevus	Sample for WB
Car-nevus-5	CAR46.01	Nevus	Sample for WB
Car-nevus-4	CAR 20.15	Blue nevus	Sample for WB and Histological slides
Car-nevus-3	CAR 742.01	Blue nevus	Histological slides
Car-lentigo-1	CAR 58.02	Benign lentigo	Histological slides
Car-lentigo-2	CAR 510.01	Benign lentigo	Histological slides

Table S4: Clinical data of CNC patients

	PRKAR1A mutation	Age	Sex	CNC associated manifestations	Hormonal data
CAR27.04	c.124C>T/p.Arg42X	Data not available	Female	Data not available	Data not available
CMC.01	Suspected somatic defect	Data not available	Male	Data not available	Data not available
CAR46.01	No mutation	46 y	Male	GH excess, thyroid nodules, LCCSCT, PPNAD, nevus	IGF-1: 410mg/mL (110-267) Free T4: 0.9ng/dL (0.7-1.5) TSH: 0.98uIU/mL (0.4-4) Testosterone: 274ng/dL (240-871) Midnight serum cortisol: 3ug/dL Prolactin: 2.5 ug/L (1-25) GH at 2 hours of OGTT: 2.8ng/mL Urinary free cortisol: 8ug/24h, 4.8ug/24h, 6.7ug/24h, and 6.8ug/24h (3.5-45)
CAR20.15	c.491_492delTG/p.Val164fsX4	32 y	Female	lentiginos, blue nevi, growth hormone excess, PPNAD, breast myxomas, pituitary adenoma, breast ductal adenoma, ovarian cyst	Midnight cortisol: 3.3 mcg/dL TSH 1.44 uIU/mL (0.4-4) Free T4 0.8 ng/dL (0.7-1.5) DHEAS 1.64 mcg/mL (18-244) GH at 2 hours of OGTT: 4.9ng/mL IGF-1 486ng/mL (110-267) FSH 4 U/L (Follicular 3-11, Midcycle 6-21, Luteal 1-9) LH <1 U/L Follicular 1-12 , Midcycle 17-77, Luteal 0-15)
CAR742.01	No mutation		Male	lentiginos, blue nevus, pigmented epithelioid melanocytoma. Patient also has a history of multiple myeloma.	Data not available
CAR58.01	Exon 2 Deletion	43 y	Female	benign lentigo, cardiac myxoma, PPNAD, hyperprolactinemia, thyroid nodules, lentiginos	Midnight serum cortisol 7.2mcg/dL FSH 7U/L (Follicular 3-11, Midcycle 6-21, Luteal 1-9) TSH 1.27mIU/mL (0.4-4) DHEAS <15ug/dL (18-244) Estradiol 79 pg/mL (15-350) ACTH 25.5 pg/mL (9-52) Thyroxine 8.4mcg/dL (4.5-12.5) LH 4 U/L Follicular 1-12 , Midcycle 17-77, Luteal 0-15) IGF-1 117ng/mL (110-267) Prolactin 30.9 mcg/L (1-25) GH at 2 hours of OGTT 0.3ng/mL
CAR510.01	No mutation	57 y	Female	benign lentigo, pituitary adenoma, GH excess, hyperprolactinemia, lentiginos. Patient also has a history of infiltrating ductal breast carcinoma and a schwannoma.	IGF-1 (post-TSS): 218ng/mL (110-267) Estradiol (post-TSS): 18 pg/mL (15-350) LH (post-TSS): 2 U/L (11-40) Free T4 (post-TSS): 1.2ng/dL (0.7-1.5) TSH (post-TSS): 0.95 uIU/mL (0.4-4) GH at 2 hours of OGTT (prior to TSS): 6.3ng/mL ACTH (post-TSS): 7pg/mL (9-52) FSH (post-TSS): 9U/L (22-153) Prolactin (post-TSS): 11ug/L (1-25) Midnight serum cortisol (post-TSS): 1.4mcg/dL UFC: 52mcg/24h and 25mcg/24h

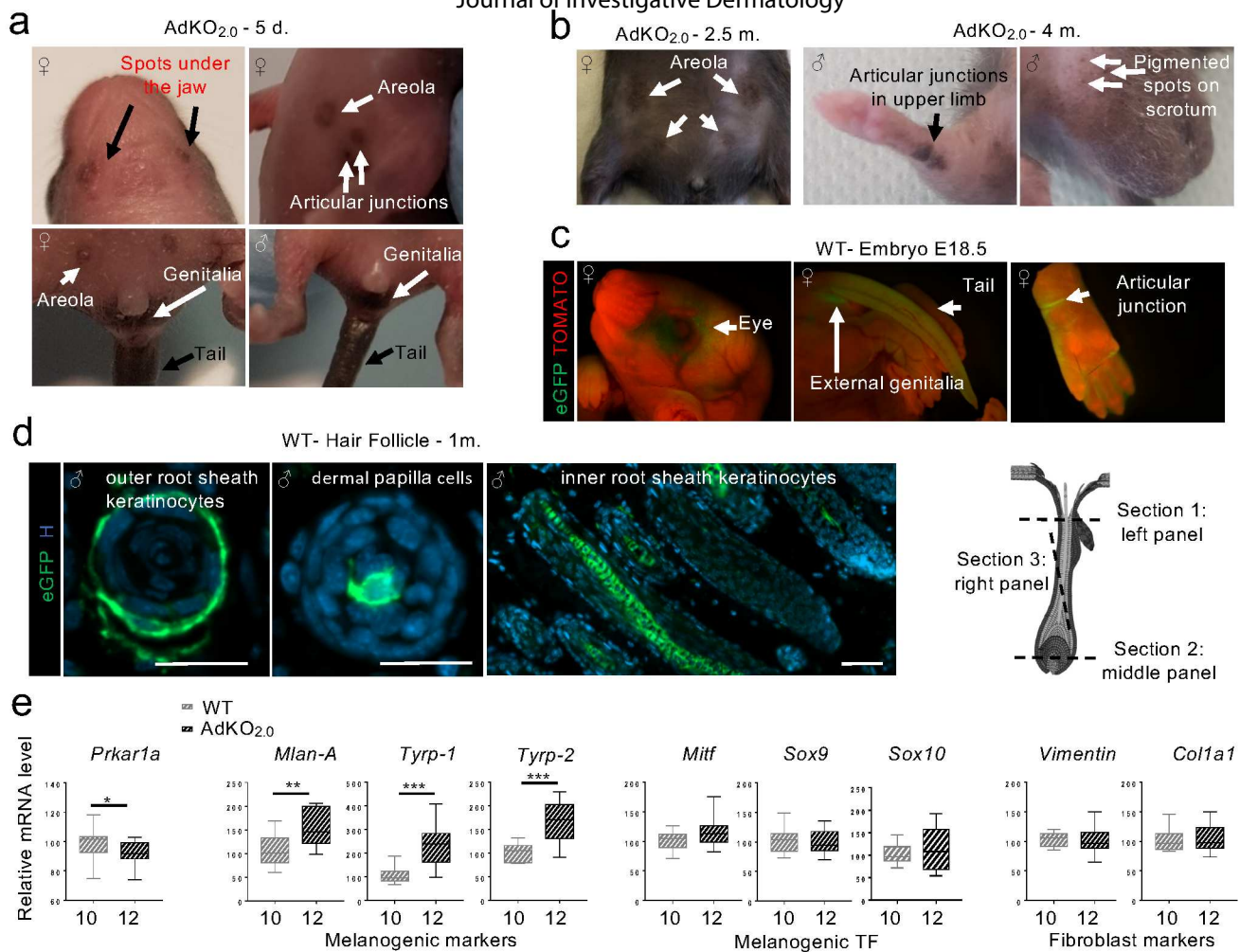


Figure S1: *Sf1*-Cre activity in AdKO_{2.0} and WT mice. a-b. Pigmentation in young (a) and adult AdKO_{2.0} mice (b). c. *Prkar1a^{fl/+}::Sf1-Cre/+::R26R^{mTmG/+}* (referred to as WT) mice allow tracking eGFP expression sites that report *Sf1*-Cre driver activity. In E18.5 embryos, direct eGFP fluorescence highlights Cre cutaneous activity (arrows). d. In various skin types, Cre is also active in hair follicles: representative picture from one-month-old WT male skin section (follicle drawing inspired from Slominski et al. 2013). Scale bars=50 μ m. e. qPCR analyses from WT and AdKO_{2.0} perigenital skins (5-day-old) confirm melanogenic markers increased expression. As expected, regarding restricted Cre activity, *Prkar1a* mRNA level is only slightly decreased in AdKO_{2.0}. mRNAs expression of melanogenic transcription factors (TF) or fibroblast markers is unchanged. N, indicated under graphs. Statistical analyses: Mann Whitney test. *P<0.05, **P<0.01, ***P<0.001.

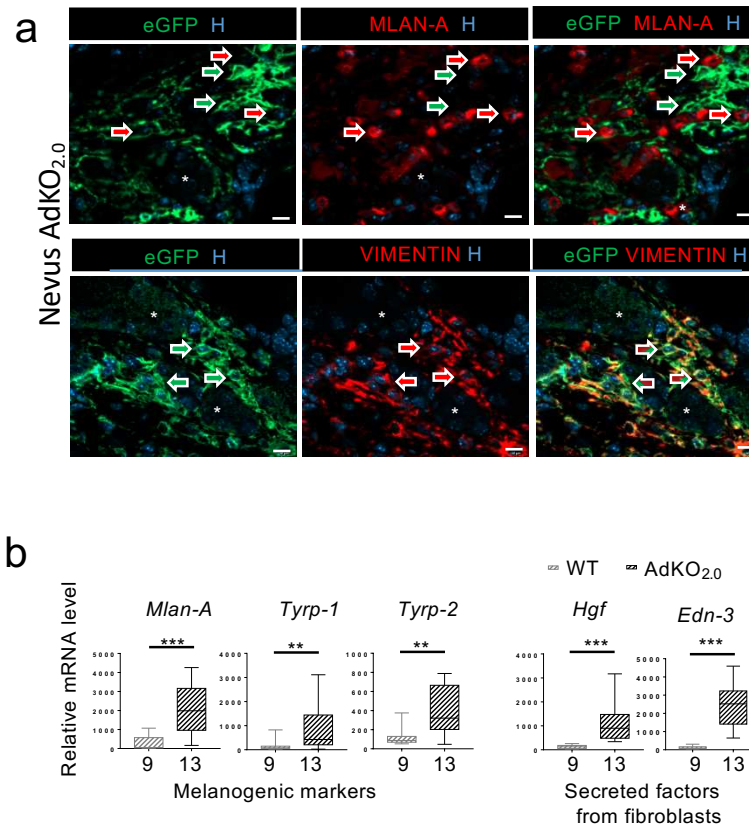


Figure S2: PKA increase affects dermal fibroblasts in AdKO_{2.0} blue nevi. a. Co-immunofluorescent labeling of eGFP (Prkar1a-KO cells, green arrows) and Melan-A (melanocytes, red arrows) in top panels, or Vimentin (mesenchymal cells, red arrows) in bottom panels, in the blue nevus shown in Figure 3a. Cells co-labelled with eGFP and Vimentin are identified by striped arrows. Hoechst nuclei staining (H). Sebaceous glands (*). Scale bars=10µm. b. qPCR analyses of melanogenic markers and fibroblastic secreted factors in WT skin (sampling located where nevi form in mutants) and AdKO_{2.0} nevi from 3-4-month-old females. N, indicated under graphs. Statistical analyses: Mann Whitney test. **P<0.01, ***P<0.001.

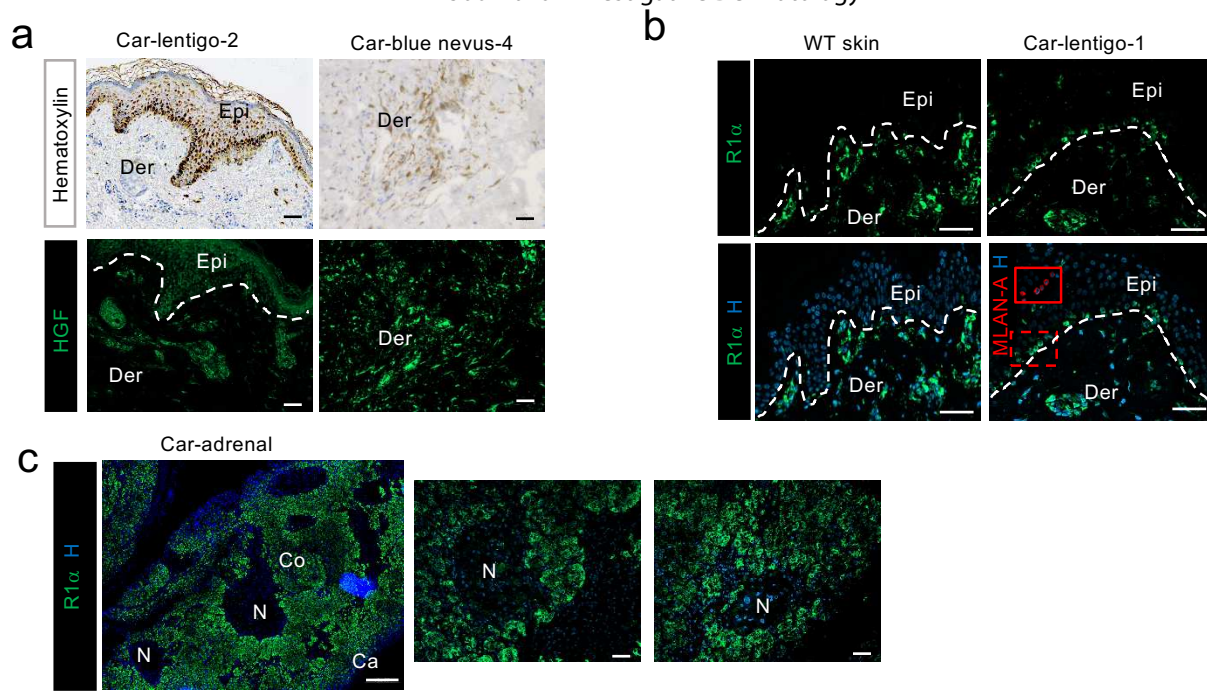


Figure S3: Lentigines, blue nevi and adrenal glands in CNC patients. a. Hematoxylin staining (black staining is melanin pigments) and immunostaining of HGF in lentigines and in blue nevus from patients with Carney complex. Scale bars=50 μ m. b. Immunofluorescent labeling of R1 α in lentigines from CNC patients. Hoechst nuclei staining (H). The red inset (corresponding to dotted red frame) shows immunolabeling of MLAN-A. Epi: Epidermis, Der: Dermis. Scale bars=50 μ m. c. Immunolabeling of R1 α in micronodular hyperplastic adrenal gland from CNC patients. Nodules (N) are negative for R1 α , confirming the specificity of the antibody. Ca, capsule; Co, cortex. Scale bars=500 μ m in the left panel and =50 μ m in the 2 right-hand panels.